

RESEARCH

Open Access



# Identification of fulvestrant analogues for estrogen receptor alpha binding in breast cancer using molecular docking and molecular dynamics simulation

Atharva Balpande<sup>1</sup>, Anushka Dashputra<sup>1</sup>, Nikhil Khanwani<sup>1</sup>, Yashasvi Therkar<sup>1</sup>, Aryan Wasewar<sup>2</sup>, Ganesh C. Patil<sup>3</sup> and C. Ravikumar<sup>4\*</sup>

\*Correspondence:

C. Ravikumar  
ravikumar@iitdh.ac.in;  
ravikumarc2006@gmail.com

<sup>1</sup>Department of Chemical Engineering, Visvesvaraya National Institute of Technology, Nagpur, India

<sup>2</sup>Department of Polymer & Surface Engineering, Institute of Chemical Technology, Mumbai, India

<sup>3</sup>Centre for VLSI and Nanotechnology, Visvesvaraya National Institute of Technology, Nagpur, India

<sup>4</sup>Department of Chemical Engineering, Indian Institute of Technology Dharwad (IIT Dharwad), Dharwad, Karnataka 580 011, India

## Abstract

Breast cancer remains a major global health challenge, with approximately 80% of cases classified as estrogen receptor-positive (ER+). Fulvestrant, a steroidal antiestrogen and selective estrogen receptor degrader (SERD), is widely used in ER+ breast cancer therapy; however, its clinical efficacy is limited by low bioavailability and resistance. In this study, we employed a computational approach to evaluate Fulvestrant analogues for their predicted interaction with the estrogen receptor alpha (ER $\alpha$ ). Molecular docking identified three analogues (9BETA,11ALPHA, 13ALPHA,14BETA,17ALPHA)-11-(METHOXYMETHYL) ESTRA-1(10),2,4-TRIENE-3,17-DIOL [EED], 2-Hydroxyestradiol, and Ethinylestradiol with more favorable binding energy (BE) values than Fulvestrant. Molecular dynamics (MD) simulations suggested that 2-Hydroxyestradiol maintains computationally stable and compact ER $\alpha$  complexes comparable to Fulvestrant, supported by hydrogen-bond analyses. Absorption, Distribution, Metabolism, Excretion, and Toxicity (ADMET) predictions indicated that Fulvestrant maintained the most favorable safety profile despite pharmacokinetic limitations, while 2-Hydroxyestradiol displayed more predictable metabolism but raised concerns of hepatotoxicity and carcinogenicity. EED and Ethinylestradiol were further constrained by significant toxicity risks. Overall, the computational evidence highlights 2-Hydroxyestradiol as a theoretically promising scaffold for further structural optimization rather than as a direct therapeutic candidate. These exclusive in-silico findings provide predictive insights for prioritizing Fulvestrant analogues; however, experimental validation through in vitro ER $\alpha$  binding, cytotoxicity assays in ER+ breast cancer cell lines, followed by in vivo studies is essential to assess clinical relevance.

**Keywords** Fulvestrant analogues, Estrogen receptor-positive breast cancer, Molecular docking, Molecular dynamics simulation, Pharmacokinetic properties

## 1 Introduction

Breast cancer remains a major global health concern and is among the leading causes of cancer-related mortality in women. In the United States, it ranks second only to lung cancer and accounts for approximately 12.5% of all newly diagnosed cancers worldwide, making it the most prevalent cancer type globally [1]. The alarming statistics reveal that about 13% (approximately one in eight) of U.S. women are expected to develop invasive breast cancer during their lifetime [2]. A substantial proportion of these cases are estrogen receptor-positive (ER+), with nearly 80% of breast tumors expressing the estrogen receptor (ER). The growth and survival of ER+ breast cancer cells are largely dependent on estrogen, which binds to the receptor and activates signaling pathways that drive tumor proliferation [3, 4]. Estrogen exerts its effects primarily through two receptor subtypes, estrogen receptor alpha (ER $\alpha$ ) and estrogen receptor beta (ER $\beta$ ). In healthy breast tissue, ER $\alpha$  is expressed in only a small subset of cells; however, its prevalence markedly increases to nearly 80% in breast cancer cells. The transcriptional activity of ER $\alpha$  is regulated by two activation domains: AF1 and AF2. AF1, located in the N-terminal domain, can be activated independently of estrogen through phosphorylation, whereas AF2, situated in the ligand-binding domain, requires estrogen binding for its activation [5–7].

Current therapeutic strategies for ER+ breast cancer largely rely on endocrine (hormonal) therapy, particularly in postmenopausal women to inhibit estrogen signaling [8, 9]. Among these therapies, Fulvestrant (Faslodex<sup>®</sup>, FDA approved) [10], a steroidal anti-estrogen has emerged as an effective treatment drug for ER+ breast cancer. Fulvestrant exerts its effects by competitively binding to ER $\alpha$ , functioning both as a selective estrogen receptor degrader (SERD) and a complete antagonist. Its binding induces a conformational change in ER $\alpha$  that disrupts AF1 and AF2-mediated transcriptional activity, while also destabilizing the receptor-ligand complex, leading to accelerated receptor degradation [11, 12]. This dual mechanism reduces ER $\alpha$  protein levels and prevents receptor dimerization and nuclear localization, thereby effectively eliminating estrogen signaling [13]. Fulvestrant exhibits a high affinity for ER $\alpha$ , approximately 89% that of estradiol, making it a potent inhibitor of estrogen-driven tumor growth [14]. Thus, Fulvestrant simultaneously binds to, blocks, and degrades ER $\alpha$ , achieving comprehensive suppression of estrogen signaling.

Despite these advantages, Fulvestrant is limited by poor bioavailability and the frequent development of tumor resistance through alternative signaling mechanisms [15]. Consequently, there is a pressing need to design novel Fulvestrant analogues with improved pharmacological profiles; particularly those that retain potent antagonistic activity without partial agonist effects, and exhibit enhanced bioavailability [16]. Figure 1a illustrates estrogen-ER $\alpha$  binding, while Fig. 1b demonstrates the competitive inhibition exerted by Fulvestrant and its analogues.

Recent efforts have increasingly focused on the discovery and characterization of Fulvestrant analogues with improved antiestrogenic activity. A key aspect of these efforts is understanding the structural features of analogues that are critical for achieving high binding affinity to ER $\alpha$  and potent antiestrogenic effects [17, 18]. Traditionally, analogues with superior binding affinity are identified through experimental ER $\alpha$  binding studies, typically involving controlled equilibrium binding assays using radiolabeled compounds [19, 20]. In contrast, computational approaches such as molecular docking, molecular dynamics (MD) simulations, and *in silico* Absorption, Distribution, Metabolism,

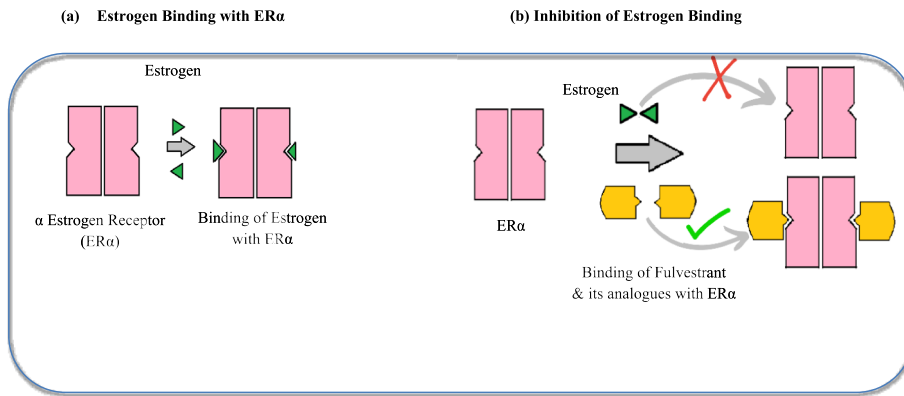


**Fig. 1** Schematic illustrating the mechanism of (a) Estrogen hormone binding to the estrogen receptor alpha (ER $\alpha$ ) and (b) competitive inhibition by Fulvestrant and its analogues, which bind to ER $\alpha$  in place of estrogen

Excretion, and Toxicity (ADMET) profiling provide efficient and robust alternatives for rapidly evaluating ligand-receptor interactions and drug-likeness. Although several SERDs and steroidal ER $\alpha$  antagonists have been explored using computational methods [21, 22], most existing studies focus on a limited set of molecules and do not integrate dynamic stability or pharmacokinetic considerations. Recent reports have highlighted the therapeutic potential of steroid-based scaffolds for ER $\alpha$  inhibition [23, 24]; however, there remains a clear gap in the systematic comparison of Fulvestrant analogues using a unified computational framework that combines molecular docking, MD simulations, and ADMET profiling. Moreover, computational studies specifically examining Fulvestrant and its structural analogues are limited [25], and further investigation is needed to elucidate how structural variations influence their interactions with ER $\alpha$ , particularly with respect to key binding moieties and engagement within the ligand-binding domain. Therefore, an integrated computational strategy is essential for identifying structurally diverse analogues with favorable binding behavior and drug-like properties, thereby enabling rational prioritization prior to experimental validation.

In the present study, we employed an integrated computational method to investigate Fulvestrant analogues with the potential to overcome current therapeutic limitations in ER+ breast cancer. Molecular docking was first performed to evaluate the binding affinities and interaction patterns of fifteen analogues with ER $\alpha$ , from which three top candidates were shortlisted. Subsequently, MD simulations were conducted to assess the structural stability, flexibility, and compactness of the ligand-ER $\alpha$  complexes. Finally, physicochemical, pharmacokinetic, and toxicity properties were evaluated through ADMET predictions to determine their suitability as drug candidates. This comprehensive in-silico assessment provides valuable insights into the therapeutic potential of Fulvestrant analogues and may facilitate the development of improved endocrine therapies for breast cancer, particularly in addressing drug resistance. Overall, the aim of this study was to identify Fulvestrant analogues with superior binding affinity and stability toward ER $\alpha$  using a unified computational framework that integrates molecular docking, MD simulations, and ADMET profiling, thereby evaluating their potential as enhanced antiestrogen agents for ER+ breast cancer.

## 2 Methodology

### 2.1 Screening of structurally similar analogues to fulvestrant

A critical step in identifying potent Fulvestrant analogues (ligands) involved screening compounds that were already reported in databases such as DrugBank and Research Collaboratory for Structural Bioinformatics Protein Data Bank (RCSB PDB). Only those analogues closely resembling Fulvestrant in structure were considered, as this targeted approach increases the likelihood of identifying ligands with higher binding affinities for ER $\alpha$ . Fulvestrant, characterized by its steroid moiety, exhibits a binding mechanism similar to estrogen, where the four hydrocarbon rings of the estradiol core establish van der Waals contacts with hydrophobic residues of ER $\alpha$  [26], while its hydroxyl groups facilitate hydrogen bonding. To select structurally relevant analogues, we employed a ligand-based screening strategy, applying a structural similarity threshold ( $\geq 0.6$  with Fulvestrant) [27].

Structural similarity values were obtained directly from the DrugBank database, which computes similarity using its built-in Tanimoto coefficient based on molecular fingerprints. These similarity values quantify the structural relatedness of each analogue to Fulvestrant. Only those ligands containing the characteristic four-ring steroid core were retained for our ligand-based screening (Table 1). Additional filters were applied to capture differences in hydroxyl group positioning and side chain substitutions, which are known to influence ER $\alpha$  binding. Our recent work has also utilized a structural similarity approach to screen analogues for different moieties [28]. Table 1 presents the list of Fulvestrant analogues including their DrugBank IDs, available RCSB PDB IDs, molecular structures, formulas, and similarity index (compared to Fulvestrant), as well as their status of usage in the study screened for evaluation of their binding affinities with the ER $\alpha$ .

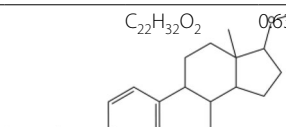
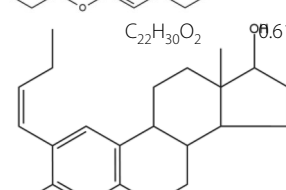
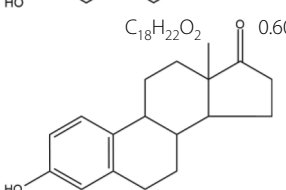
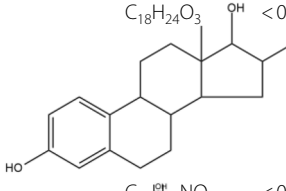
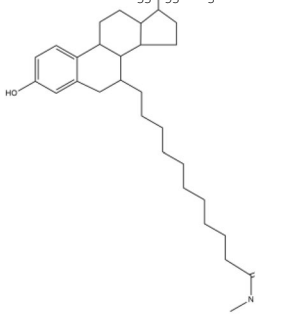
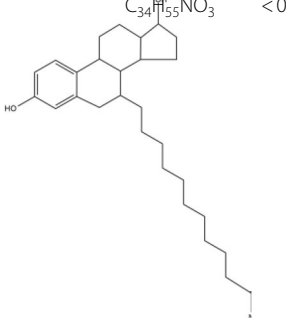
### 2.2 Molecular docking studies

Molecular docking serves as a crucial tool in identifying favorable interactions within protein–ligand or protein–protein complexes, primarily based on their binding affinity. It predicts how the ligands or proteins fit into protein pockets of the receptor and the strength of their binding, forming a complex [29]. In addition, molecular docking provides insights into the types of interactions involved, such as van der Waals forces, hydrogen bonds, amide bonds, and  $\pi$ -interactions, as well as the amino acid residues responsible for binding [30]. In this study, molecular docking was performed for all screened ligands (Table 1) with the ER $\alpha$  using AutoDock 4.2.6 to calculate their binding energies (BE, kcal/mol), where more negative BE values indicate stronger predicted binding. Ligand structure data files (SDF) were retrieved from the DrugBank and RCSB PDB databases and converted to PDBQT format using Open Babel 2.4.1. The receptor structure (PDB ID: 1X7E) was prepared by removing crystallographic water molecules to prevent non-biological interactions, repairing missing atoms, adding polar hydrogens, and assigning and redistributing Kollman charges. Ligands were introduced by detecting the torsion root. To avoid bias in binding-site selection, blind docking was conducted using a grid box sufficiently large to cover the entire receptor ( $126 \times 126 \times 126$  points,  $0.375 \text{ \AA}$  spacing, centered at  $X = 41.752$ ,  $Y = 25.913$ ,  $Z = 23.614$ ) [30, 31]. Docked poses were clustered using a  $2.0 \text{ \AA}$  root mean square deviation (RMSD) threshold. The docking results consistently revealed that the ligands bound to the same site as the

**Table 1** Fulvestrant analogues (ligands) screened for evaluating their binding affinities with estrogen receptor alpha (ER $\alpha$ )

S. No	Ligand name [with DrugBank (DB) and RCSB PDB IDs]	Molecular structure	Molecular formula	Similarity index	Status
1	2-Hydroxyestradiol (DB ID: DB07706) (PDB ID: ECS)		C <sub>18</sub> H <sub>24</sub> O <sub>3</sub>	0.71	Mod- eled
2	Ethinylestradiol (DB ID: DB00977) (PDB ID: 3WF)		C <sub>20</sub> H <sub>24</sub> O <sub>2</sub>	0.693	Mod- eled
3	(9BETA,11ALPHA,13ALPHA,14BETA,17ALPHA)-11-(METHOXYMETHYL) ESTRA-1(10),2,4-TRIENE-3,17-DIOL [EED] (DB ID: DB07707) (PDB ID: EED)		C <sub>20</sub> H <sub>28</sub> O <sub>3</sub>	0.66	Mod- eled
4	Fluoroestradiol F-18 (DB ID: DB15690)		C <sub>18</sub> H <sub>23</sub> FO <sub>2</sub>	0.735	Eli- gible
5	Estriol (DB ID: DB04573) (PDB ID: ESL)		C <sub>18</sub> H <sub>24</sub> O <sub>3</sub>	0.718	Eli- gible
6	Estetrol (DB ID: DB12235) (PDB ID: 4OH)		C <sub>18</sub> H <sub>24</sub> O <sub>4</sub>	0.696	Eli- gible
7	Epimestrol (DB ID: DB13386)		C <sub>19</sub> H <sub>26</sub> O <sub>3</sub>	0.688	Eli- gible
8	2-Methoxyestradiol (DB ID: DB02342) (PDB ID: ESM)		C <sub>19</sub> H <sub>26</sub> O <sub>3</sub>	0.683	Eli- gible
9	Mestranol (DB ID: DB01357)		C <sub>21</sub> H <sub>26</sub> O <sub>2</sub>	0.66	Eli- gible

**Table 1** (continued)

S. No	Ligand name [with DrugBank (DB) and RCSB PDB IDs]	Molecular structure	Molecular formula	Similarity index	Status
10	Promestriene (DB ID: DB12487)		C <sub>22</sub> H <sub>32</sub> O <sub>2</sub>	0.635	Eli- gible
11	(9ALPHA,13BETA,17BETA)-2-[(1Z)-BUT-1-EN-1-YL]ESTRA-1,3,5(10)-TRIENE-3,17-DIOL (DB ID: DB07678) (PDB ID: DRQ)		C <sub>22</sub> H <sub>30</sub> O <sub>2</sub>	0.61	Eli- gible
12	Estrone (DB ID: DB00655) (PDB ID: J3Z)		C <sub>18</sub> H <sub>22</sub> O <sub>2</sub>	0.607	Eli- gible
13	(16ALPHA,17ALPHA)-ESTRA-1,3,5(10)-TRIENE-3,16,17-TRIOL (DB ID: DB07702) (PDB ID: E3O)		C <sub>18</sub> H <sub>24</sub> O <sub>3</sub>	< 0.6	Not eli- gible
14	11-[3,17beta-dihydroxyestra-1,3,5(10)-trien-7beta-yl]-N-methyl-N-propylundecanamide (DB ID: DB01069) (PDB ID: 3YJ)		C <sub>33</sub> H <sub>53</sub> NO <sub>3</sub>	< 0.6	Not eli- gible
15	N-BUTYL-11-[(7R,8R,9S,13S,14S,17S)-3,17-DIHYDROXY-13-METHYL-7,8,9,11,12,13,14,15,16,17-DECAHYDRO-6H-CYCLOPENTA[A]PHENANTHREN-7-YL]-N-METHYLUNDECANAMIDE (DB ID: DB03860) (PDB ID: AOE)		C <sub>34</sub> H <sub>55</sub> NO <sub>3</sub>	< 0.6	Not eli- gible

**Table 1** (continued)

S. No	Ligand name [with DrugBank (DB) and RCSB PDB IDs]	Molecular structure	Molecular formula	Similarity index	Status
16	Fulvestrant (DB ID: DB00947) (PDB ID: FVS)		C <sub>32</sub> H <sub>47</sub> F <sub>5</sub> O <sub>3</sub> S	1	Base

**Table 2** Summary of docking parameters used for AutoDock 4.2.6 simulations of ERα-ligand complexes

Parameter	Description/value
Software	AutoDock 4.2.6
Ligand preparation	Structures retrieved from RCSB PDB / DrugBank; converted from SDF to PDBQT using Open Babel 2.4.1
Estrogen receptor alpha (ERα)	PDB ID: 1X7E (co-crystallized ligand removed; polar hydrogens added; Kollman charges assigned)
Docking type	Blind docking (covering entire receptor)
Grid Box dimensions	126 × 126 × 126 points
Grid spacing	0.375 Å
Algorithm	Lamarckian Genetic Algorithm (GA)
Number of GA runs	50
Population size	300
Maximum number of evaluations	2.5 × 10 <sup>6</sup>
Maximum number of generations	27,000
Energy evaluations	50,000 steps per run
Output/Analysis tools	BIOVIA Discovery Studio Visualizer 2020 for visualization and interaction mapping

co-crystallized ligand, corresponding to the experimentally validated ligand-binding domain of ERα. Although an overlay image could not be included, blind docking consistently reproduced the experimentally validated co-crystallized binding site, as evidenced by the alignment of key residues (GLU353, ARG394, PHE404, and GLY521) across all top-ranked poses (Table 3).

Molecular docking was performed using the Lamarckian Genetic Algorithm (LGA) with the following settings: 50 GA runs, a population size of 300, a mutation rate of 0.02, a crossover rate of 0.8, and 2–25 million energy evaluations. The AutoDock scoring function, which incorporates van der Waals, electrostatic, hydrogen bonding, and desolvation terms, was used to compute BE values. Although 2D interaction diagrams do not explicitly display van der Waals contacts, these interactions are fully accounted for in the AutoDock 4.2.6 scoring function. Docking results were visualized using BIOVIA Discovery Studio Visualizer, and the three ligands with the most favorable BE values were selected for MD simulations (as described in Sect. 2.1).

All docking parameters used in this study are summarized in Table 2, and the overall docking workflow is illustrated in Fig. 2. It should be noted that in AutoDock 4.2.6, the BE values are calculated using a scoring function that integrates van der Waals, electrostatic, hydrogen bonding, and desolvation contributions. Thus, van der Waals

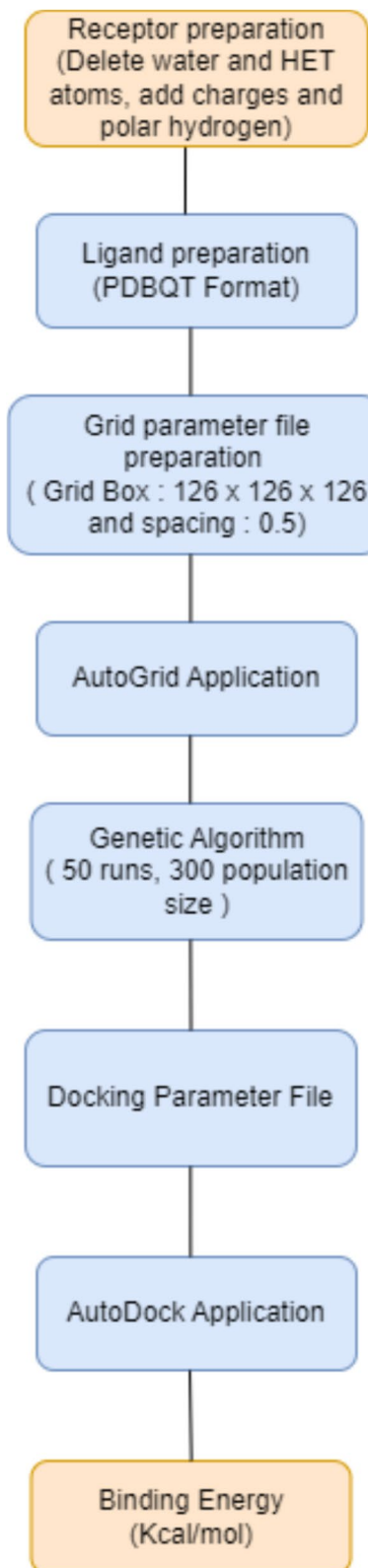


**Fig. 2** Flowchart illustrating the steps involved in the molecular docking simulation

interactions were inherently considered in the docking calculations, even though they are not displayed separately in the 2D interaction diagrams generated with BIOVIA Discovery Studio Visualizer.

### 2.3 Visualization of docking poses and interactions of ER $\alpha$ -ligand complex

Visualization of docking poses is essential for interpreting molecular interactions and validating docking results. These graphical analyses provide insights into the orientation of ligands within the receptor binding site and the types of interactions that stabilize the complexes[32]. In this study, the docking poses of ER $\alpha$  with its ligands were examined to evaluate binding efficacy and interaction profiles. The conformations with the lowest BE values for each ER $\alpha$ -ligand complex were extracted from AutoDock output files (PDBQT format) and converted to PDB format using Open Babel 2.4.1 [33]. These structures were then imported into BIOVIA Discovery Studio Visualizer[34], where receptor and ligand definitions were assigned. Receptor surfaces were visualized to highlight hydrogen bonds, bond distances were measured, and 2D interaction diagrams were generated to display hydrogen bonds,  $\pi$ -interactions, and other contacts between amino acid residues and the ligand. This visualization approach provides a detailed picture of the molecular interactions underlying docking outcomes and facilitates a better understanding of the binding mode of Fulvestrant analogues.

### 2.4 MD simulation of various ER $\alpha$ -ligand complexes

MD simulation is a powerful computational approach for investigating the structural behavior of biomolecules and their interactions with ligands over time. By capturing atomic movements and conformational changes, MD simulation provides valuable insights into protein stability, flexibility, and binding mechanisms, making it an essential tool in modern drug discovery [35]. In this study, MD simulations of the ER $\alpha$ -ligand complexes were performed using GROMACS 2022.3 with the CHARMM36m force field. Ligand topologies were generated using CGenFF (v4.6) and converted to GROMACS format using *cgenff\_charmm2gmx.py* [36]. Each complex was solvated in a dodecahedral TIP3P water box with 1.0 nm padding, neutralized, and adjusted to 0.15 M NaCl, and the topology file of complex was created.

A positional restraint parameter was included to provide stable relaxation and prevent ligand from drifting away from the binding site. Energy minimization was performed using the steepest-descent algorithm (50,000 steps). Equilibration consisted of 100 ps NVT (310 K, Berendsen thermostat) through *gmx mdrun -deffnm nvt* module followed by 100 ps NPT (1 bar, Parrinello-Rahman barostat) using *gmx mdrun -deffnm npt* module. Thermostat is applied to the coupled system of protein and ligand to prevent system blow up. Production MD simulations were run for 50 ns per replica (three replicas) using a 2 fs timestep, NPT ensemble, Nosé-Hoover thermostat (310 K), Parrinello-Rahman barostat, PME electrostatics, 1.2 nm cutoffs, and LINCS constraints [31] on all bonds. Trajectory analyses [RMSD, root mean square fluctuation (RMSF), and radius of gyration (Rg)] were performed using GROMACS tools. The overall workflow for MD simulations is summarized in Fig. 3.

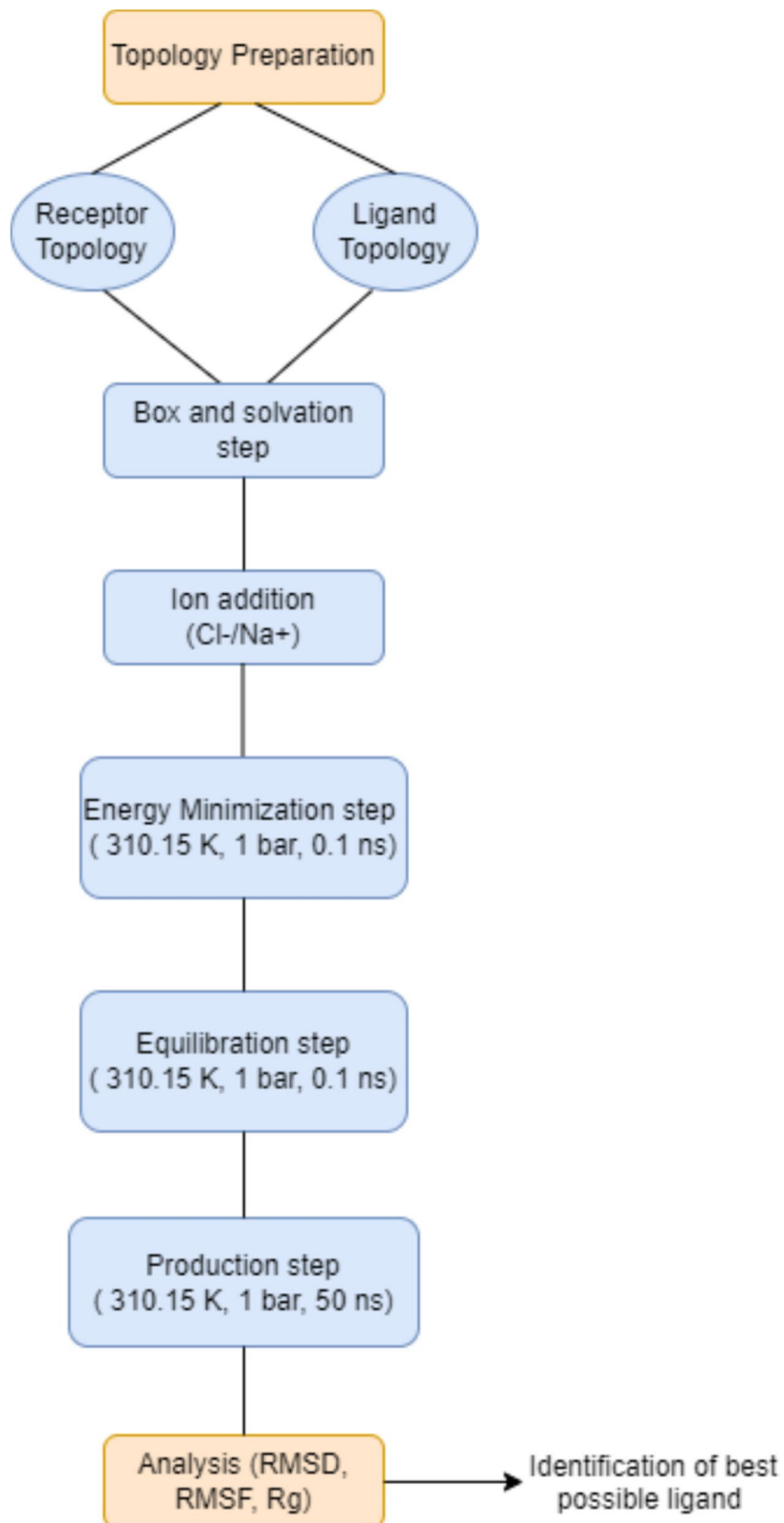


**Fig. 3** Flowchart illustrating the sequential steps followed in the MD simulation procedure

## 2.5 Hydrogen bonding analysis

Hydrogen bonding is a key factor in stabilizing protein–ligand interactions and strongly influences binding affinity [37]. Therefore, during MD simulations, we analyzed the formation and persistence of hydrogen bonds within each ligand-ER $\alpha$  complex. This evaluation provided insights into the specificity of ligand binding and the overall stability of the complexes throughout the simulation trajectory. The number and occupancy of hydrogen bonds were quantified using the 'gmx hbond' command in GROMACS, which calculates hydrogen bond formation between protein residues and ligands over the course of the simulation. Hydrogen bonds were identified using the *gmx hbond* module in GROMACS, applying a donor–acceptor distance cutoff of  $\leq 3.5$  Å (0.35 nm) and a donor-hydrogen-acceptor angle cutoff of  $\leq 30^\circ$ , which correspond to the default criteria for hydrogen-bond detection in GROMACS.

## 2.6 ADMET analysis of ligands

ADMET analysis was performed to evaluate the physicochemical and pharmacokinetic properties of the screened ligands using ADMETlab 3.0 software (accessed April 29, 2025) [38, 39]. By comprehensively assessing these factors, ADMET studies provide insights into drug–body interactions and help minimize the risk of adverse effects [40, 41]. The physicochemical parameters analyzed included molecular weight (MW), number of rings (nRing), formal charge (fChar), number of heteroatoms (nHet), size of the largest ring (MaxRing), number of rotatable bonds (nRot), topological polar surface area (TPSA), number of hydrogen bond donors (nHD), number of hydrogen bond acceptors (nHA), distribution coefficient (logD), solubility (logS), and partition coefficient (logP). The pharmacokinetic properties evaluated included Human intestinal absorption (HIA), volume of distribution (VD), blood–brain barrier (BBB) penetration, plasma protein binding (PPB), cytochrome (CYP) inhibition/substrate profiles, excretion, and toxicity (AMES mutagenicity, hepatotoxicity, and carcinogenicity) prediction. These analyses provide a comprehensive evaluation of the drug-likeness, pharmacological behavior, and potential risks associated with the selected ligands, supporting their assessment as Fulvestrant analogues.

## 3 Results and discussions

### 3.1 Molecular docking studies

All the ligands (listed in Table 1) were docked with the ER $\alpha$ , and their BE values were calculated. The BE values were used to identify ligands with stronger binding affinities for ER $\alpha$  compared to Fulvestrant, where a more negative BE value indicates stronger binding affinity [34]. Table 3 presents the ligands ranked according to their BE values, with several ligands exhibiting docking scores close to -10 kcal/mol. Among these, the top three ligands with the most negative BE values were (9BETA,11ALPHA,13ALPHA,14BETA,17ALPHA)-11-(METHOXYMETHYL) ESTRA-1(10),2,4-TRIENE-3,17-DIOL [EED], 2-Hydroxyestradiol, and Ethinylestradiol, with respective BE values of -10.80, -10.63, and -10.36 kcal/mol, all of which are substantially more negative than that of Fulvestrant (-6.49 kcal/mol) (Table 3), suggesting that these analogues could serve as potential alternatives for inhibiting estrogen binding to ER $\alpha$ .

A BE of approximately -10 kcal/mol typically reflects a strong and stable receptor-ligand interaction, indicating that these ligands may possess substantial inhibitory

**Table 3** Binding energy (BE) values obtained from molecular docking of Fulvestrant analogues (ligands) with the estrogen receptor alpha (ER $\alpha$ ) in ER+ breast cancer cells

S.No	Ligand name	Binding energy, BE (kcal/mol)
1	(9BETA,11ALPHA,13ALPHA,14BETA,17ALPHA)-11-(METHOXYMETHYL) ESTRA-1(10),2,4-TRIENE-3,17-DIOL (EED)	-10.80
2	2-Hydroxyestradiol	-10.63
3	Ethinylestradiol	-10.36
4	Fluoroestradiol F-18	-10.34
5	(16ALPHA,17ALPHA)-ESTRA-1,3,5(10)-TRIENE-3,16,17-TRIOL	-10.30
6	Epimestrol	-10.20
7	Estriol	-10.01
8	Estetrol	-9.76
9	Mestranol	-9.71
10	2-Methoxyestradiol	-9.20
11	Promestriene	-9.05
12	(9ALPHA,13BETA,17BETA)-2-[(1Z)-BUT-1-EN-1-YL] ESTRA-1,3,5(10)-TRIENE-3,17-DIOL	-8.98
13	Estrone	-8.59
14	11-[3,17beta-dihydroxyestra-1,3,5(10)-trien-7beta-yl]-N-methyl-N-propylundecanamide	-8.13
15	N-BUTYL-11-[(7R,8R,9S,13S,14S,17S)-3,17-DIHYDROXY-13-METHYL-7,8,9,11,12,13,14,15,16,17-DECAHYDRO-6H-CYCLOPENTA[A]PHENANTHREN-7-YL]-N-METHYLUNDECANAMIDE	-7.87
16	Fulvestrant	-6.49

potential toward ER $\alpha$ . These analogues exhibit approximately 40–60% stronger binding affinity than Fulvestrant, based on the proportional difference between their BE values and that of Fulvestrant. Although nearly seven ligands demonstrated BE values close to -10 kcal/mol, we selected only the top three EED, 2-Hydroxyestradiol, and Ethinylestradiol for further MD simulation and ADMET analysis. The selection was based on their superior ranking in docking energies, they represent structurally diverse modifications of the estradiol scaffold (including a methoxy-substituted analogue, a hydroxylated analogue, and a synthetic estrogen analogue), enabling us to explore different chemical variations in relation to ER $\alpha$  binding, and the computational feasibility of conducting detailed simulations. Additionally, preliminary drug-likeness screening (Sect. 3.3) suggested that these three ligands possessed more favorable physicochemical properties compared to the other candidates with similar docking scores. Furthermore, the other ligands with comparable docking scores were unsuitable for therapeutic repurposing; for example, Fluoroestradiol F-18 is an FDA-approved diagnostic radiotracer rather than a drug candidate, and therefore was excluded from further analysis[42].

Figures 4, 5, 6, 7 showcase the docked poses of the selected ligands EED, 2-Hydroxyestradiol, Ethinylestradiol, and Fulvestrant with the ER $\alpha$ . The numerical values provided represent the bond lengths associated with the formed bonds. Additionally, these figures present a 2D plot depicting interactions with surrounding amino acid residues. It should be noted that van der Waals interactions were inherently accounted in the docking BEs by AutoDock 4.2.6. Table 4 illustrates the type of interactions and the amino acid residues involved during complex formation. The docking protocol was validated by redocking the co-crystallized ligand, which reproduced the experimental pose with an RMSD < 2 Å, confirming the reliability of the docking procedure.

The strong BEs observed for EED, 2-Hydroxyestradiol, and Ethinylestradiol suggest that structural modifications to the steroid scaffold can significantly enhance ER $\alpha$

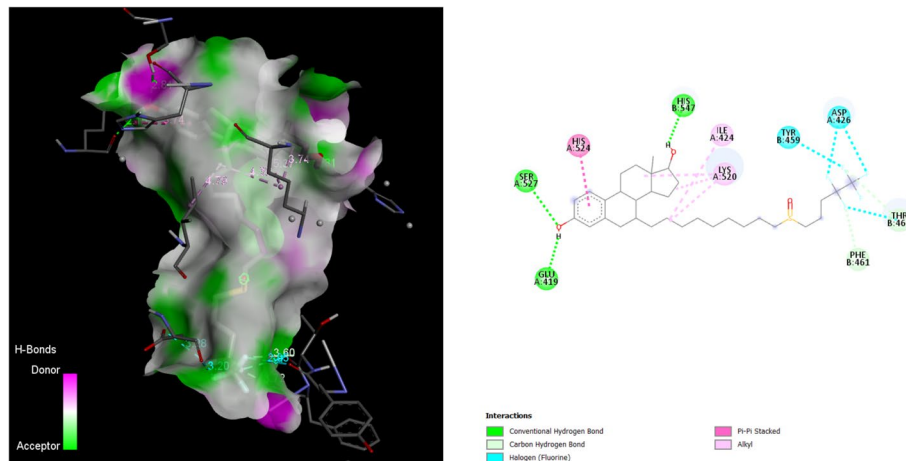


**Fig. 4** Binding poses of Fulvestrant with ER $\alpha$  showing the corresponding bond distances, along with a 2D representation depicting the interactions with key amino acid residues

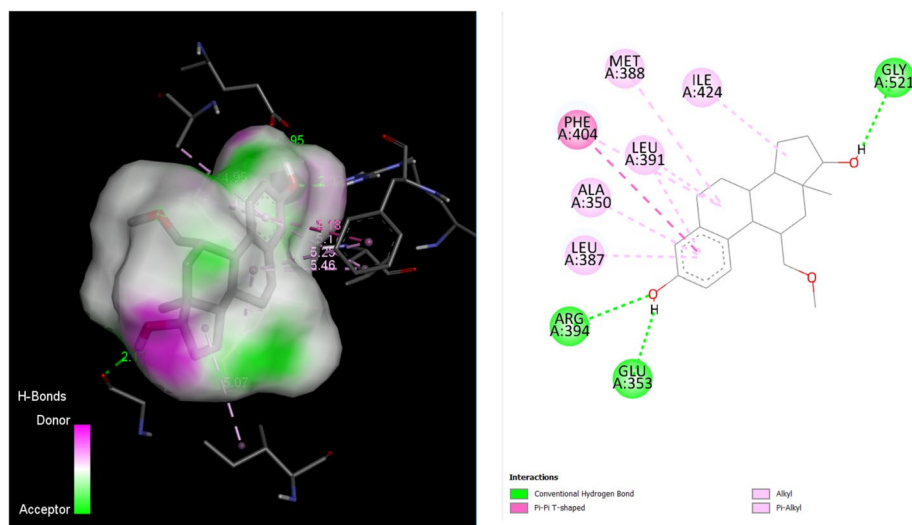


**Fig. 5** Binding poses of EED with ER $\alpha$  showing the corresponding bond distances, along with a 2D representation depicting the interactions with key amino acid residues

affinity. In particular, hydroxyl substitutions are known to facilitate hydrogen bonding within the ligand-binding domain (LBD), while bulky substituents contribute to hydrophobic stabilization [38]. This is consistent with our observation that 2-Hydroxyestradiol achieved docking energies comparable to or better than Fulvestrant. Previous studies have similarly reported that hydroxylated estradiol derivatives can retain high ER $\alpha$  affinity, supporting their potential as antiestrogenic analogues [39]. Thus, docking results provide a rationale for prioritizing these analogues for dynamic stability analysis.

The detailed analysis of the binding poses and interactions reveal that these top ligands form extensive and diverse interactions with the ER $\alpha$ , contributing to their high binding affinities. Table 4 illustrate that EED ligand with the most negative BE value, interacts with amino acids ARG A:394, GLU A:353, and GLY A:521 through conventional hydrogen bonds, and with PHE A:404 through pi-pi interactions, among other hydrophobic interactions. Similarly, 2-Hydroxyestradiol and Ethinylestradiol exhibited strong binding through multiple conventional hydrogen bonds with GLY A:521, GLU A:353, and

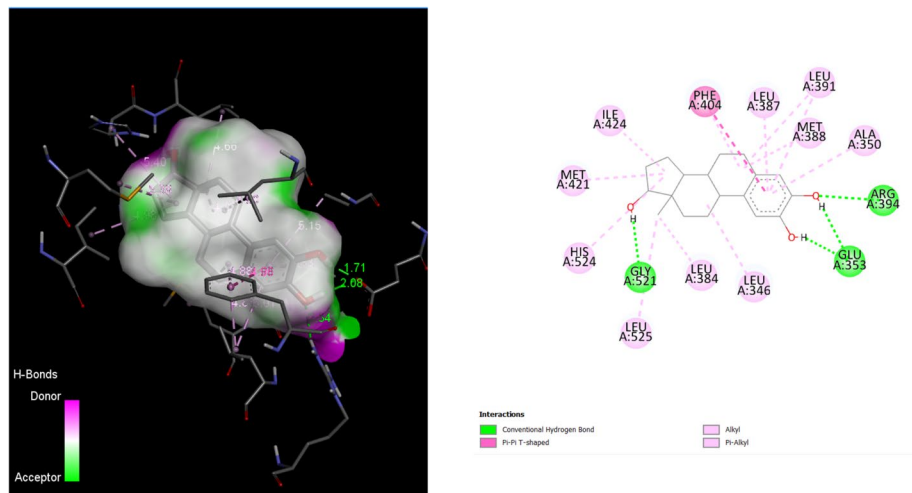


**Fig. 6** Binding poses of 2-Hydroxyestradiol with ER $\alpha$  showing the corresponding bond distances, along with a 2D representation depicting the interactions with key amino acid residues

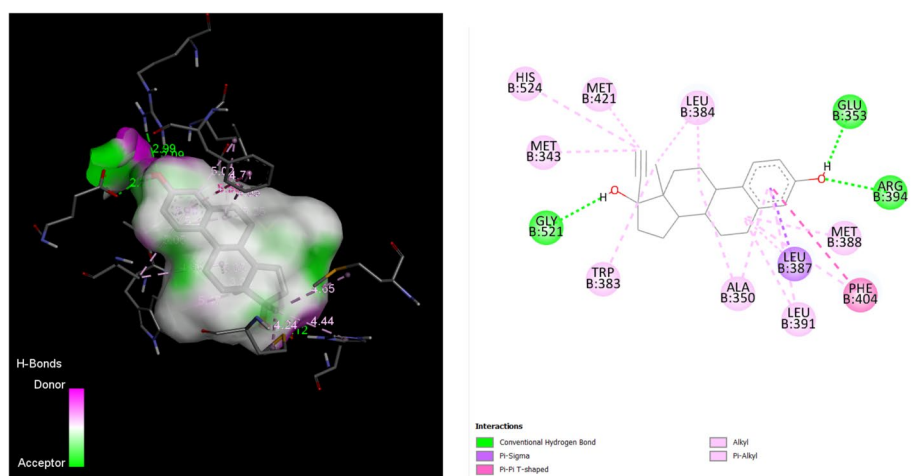


**Fig. 7** Binding poses of Ethinylestradiol with ER $\alpha$  showing the corresponding bond distances, along with a 2D representation depicting the interactions with key amino acid residues

ARG A:394, and pi-pi interactions with PHE A:404, in addition to several alkyl interactions stabilizing the ligand within the receptor binding site. In comparison, Fulvestrant, although an effective ER $\alpha$  antagonist in clinical settings, demonstrated fewer and less diverse interactions, leading to a higher (less negative) BE value. Fulvestrant primarily interacted with residues SER A:527, GLU A:419, and HIS B:547 through hydrogen bonds, and with HIS A:524 through pi-pi interactions, along with limited alkyl interactions. The significant binding affinities of EED, 2-Hydroxyestradiol, and Ethinylestradiol, as evidenced by their strong interactions and more negative BE values, suggest their potential as promising alternatives to Fulvestrant for inhibiting estrogen binding to ER $\alpha$  in ER+ breast cancer cells. These findings indicate that further studies, including MD simulations, are necessary to explore their compactness, stability, flexibility behavior during the complex formation with the ER $\alpha$ .

**Table 4** Amino acid residues of estrogen receptor alpha (ER $\alpha$ ) involved in interactions with the ligands EED, 2-Hydroxyestradiol, Ethinylestradiol, and Fulvestrant, classified according to the type of molecular interaction

Sr. No	Ligand	Amino acid residues of ER $\alpha$ classified based on the type of bonds				
		Conventional Hbond	Carbon Hbond	Pi-Pi	Alkyl	Pi-sigma
1	(9BETA,11ALPHA,13ALPHA,14BETA,17ALPHA)-11-(METHOXYMETHYL)ESTRA-1(10),2,3,17-TRIENE-3,17-DIOL (EED)	ARG A:394, GLU A:353, GLY A:521	—	PHE A:404	MET A:388, ILE A:424, LEU A:391, ALA A:350, LEU A:387	—
2	2-Hydroxyestradiol	GLY A:521, GLU A:353, ARG A:394	—	PHE A:404	ILE A:424, MET A:421, HIS A:524, LEU A:525, LEU A:387, LEU A:391, MET A:388, LEU A:384, LEU A:346, ALA A:350	—
3	Ethinylestradiol	GLY A:521, GLU A:353, ARG A:394	—	PHE A:404	HIS B:524, MET B:421, MET B:343, TRP B:383, LEU B:384, ALA B:350, LEU B:391, MET B:388	LEU B:387
4	Fulvestrant	SER A:527, GLU A:419, HIS B:547	THR B:460, PHE B:461	HIS A:524	ILE A:424, LYS A:520	—

### 3.2 MD simulation studies

To better understand the dynamic interactions between the selected ligands and the ER $\alpha$ , MD simulations were performed for the ER $\alpha$  complexes with EED, 2-Hydroxyestradiol, Ethinylestradiol, and Fulvestrant. These ligands were prioritized for simulation on the basis of their docking results, where each demonstrated significantly more negative BE values compared to the ER $\alpha$ -Fulvestrant complex. The aim of MD simulations was to assess structural stability, flexibility, and compactness of the complexes over time, thereby offering insights into the mechanisms by which these ligands may function as potential Fulvestrant analogues. To achieve this, RMSD plots were generated to monitor structural deviations of the ligands during their interaction with the ER $\alpha$ . RMSF plots were employed to evaluate residue-level flexibility, and Rg plots were analyzed to assess overall compactness of the complexes. The ER $\alpha$ -Fulvestrant complex was used as the reference standard for comparison.

RMSD trajectories (Fig. 8a) revealed clear differences in complex stability among the ligands. The ER $\alpha$ -Fulvestrant (black) and ER $\alpha$ -2-Hydroxyestradiol (green) complexes exhibited low RMSD values (low fluctuations), remaining within the accepted range of 0.1–0.5 nm [43] throughout the simulation, which indicates strong conformational stability and robust binding. In contrast, the complexes with EED and Ethinylestradiol showed higher RMSD values and larger deviations, pointing to moderate stability and greater conformational perturbations during the simulation.

These observations suggest that 2-Hydroxyestradiol forms a stable complex with ER $\alpha$ , comparable to Fulvestrant, whereas EED and Ethinylestradiol fail to achieve similar stability. RMSF analysis (Fig. 8b) provided residue-level insights into protein flexibility [35]. All four complexes displayed multiple peaks, reflecting localized fluctuations within the ER $\alpha$  structure during ligand binding. The overall similarity in RMSF profiles across Fulvestrant and its analogues indicates that each ligand effectively engages with the ER $\alpha$

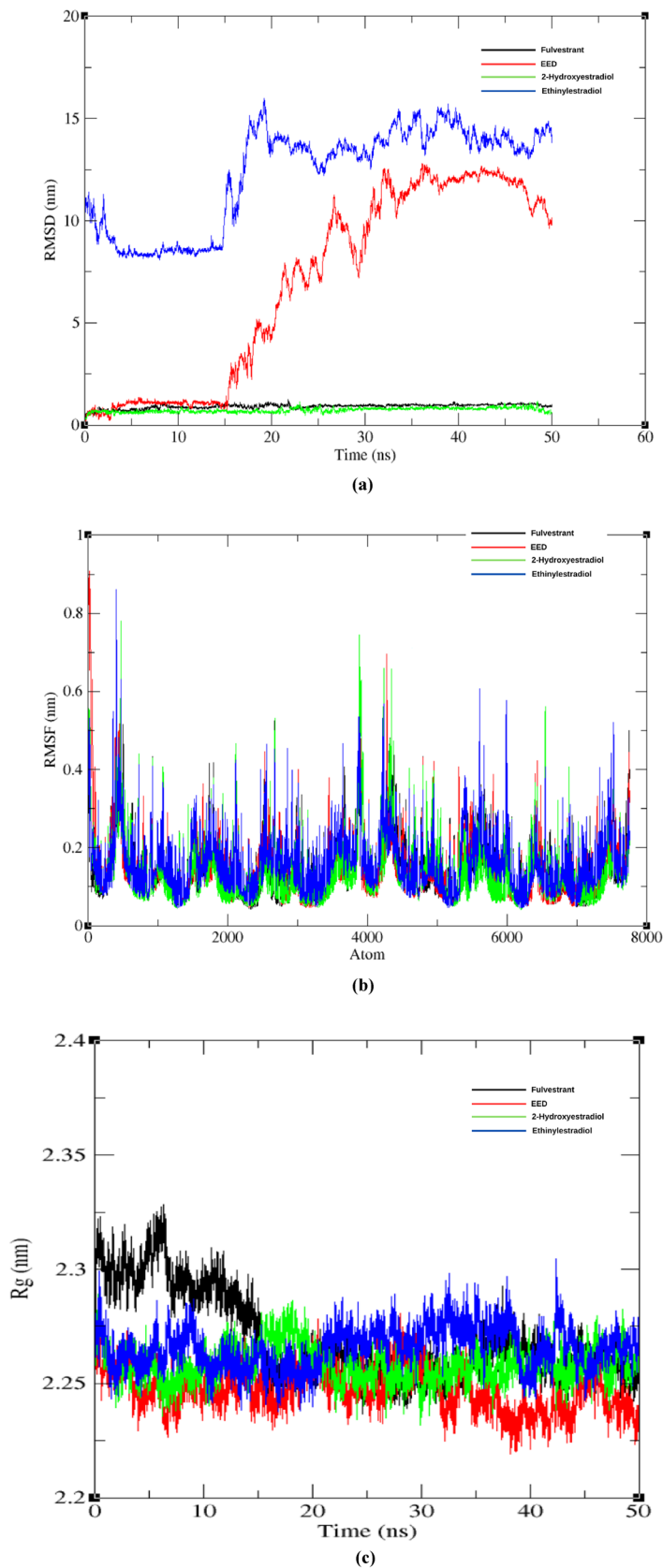


**Fig. 8** **a** Root mean square deviation (RMSD), **b** root mean square fluctuation (RMSF), and **c** radius of gyration ( $R_g$ ) trajectories of EED, 2-Hydroxyestradiol, Ethinylestradiol, and Fulvestrant during their complex formation with ER $\alpha$

binding pocket. However, higher peaks in certain regions for EED and Ethinylestradiol suggest that their interactions induce more pronounced flexibility, consistent with their less stable RMSD profiles. The  $R_g$  plots (Fig. 8c) offered further validation of complex stability by assessing compactness. A consistent range of  $R_g$  values throughout the simulation duration suggests the compactness of the formed complexes. For all four ligands,  $R_g$  values remained relatively stable within the range of 2.26–2.36 nm [44], signifying uniform distribution of atoms and preservation of ER $\alpha$  structural integrity. These results indicate that all complexes achieved compact conformations without loss of protein function.

The MD simulation studies collectively demonstrate that 2-Hydroxyestradiol closely resembles Fulvestrant in terms of RMSD, RMSF, and  $R_g$  parameters, forming a stable, compact, and flexible complex with ER $\alpha$ . This stability is likely attributable to its ability to form consistent hydrogen bonds and maintain tight protein–ligand packing, features that contribute to effective receptor engagement. In contrast, EED and Ethinylestradiol exhibited higher RMSD values and greater fluctuations, suggesting reduced stability and less favorable binding dynamics. Such differences are important, as MD simulations capture conformational changes that are often overlooked in docking-only studies. Similar computational analyses of estradiol derivatives have demonstrated that dynamic stability is a key determinant of antagonist potential[45]. These findings reinforce that 2-Hydroxyestradiol may serve as a more reliable analogue for further investigation.

Hydrogen bonding plays a critical role in stabilizing protein–ligand complexes, with higher hydrogen bond occupancy generally correlating with stronger binding affinity and increased stability [46–48]. In this study, the dynamics of hydrogen bond interactions between ER $\alpha$  and the ligands were assessed throughout the MD simulation. Figure 9a–d illustrates the number and stability of hydrogen bonds formed in complexes with Fulvestrant, EED, 2-Hydroxyestradiol, and Ethinylestradiol, respectively. For the reference complex, ER $\alpha$ -Fulvestrant (Fig. 9a), hydrogen bond interactions fluctuated dynamically across the simulation, and consistently exhibited high occupancy, with multiple bonds forming simultaneously at several intervals.

This indicates that Fulvestrant maintains stable and robust interactions with ER $\alpha$ , consistent with its role as a potent estrogen receptor antagonist. In comparison, the ER $\alpha$ -EED complex (Fig. 9b) displayed fewer hydrogen bonds, with frequent intervals of no hydrogen bond formation, reflecting lower occupancy and reduced stability. This suggests a weaker binding affinity of EED, which may compromise its biological activity. The ER $\alpha$ -2-Hydroxyestradiol complex (Fig. 9c) demonstrated hydrogen bond interactions nearly equivalent to Fulvestrant, with consistent formation reflected by short fluctuations. This pattern implies that 2-Hydroxyestradiol forms stable hydrogen bonds with ER $\alpha$ , supporting its potential as a Fulvestrant analogue. The ER $\alpha$ -Ethinylestradiol complex (Fig. 9d) exhibited moderate hydrogen bond formation, with stable interactions interspersed by fluctuations, indicative of moderate binding affinity and dynamic stability within the complex. Comparatively, Fulvestrant exhibited the highest and most stable hydrogen bond occupancy, while EED showed the lowest, suggesting limited binding strength. 2-Hydroxyestradiol consistently displayed hydrogen bond interactions comparable to Fulvestrant, supporting its strong binding potential. Overall, these results reinforce the notion that stable hydrogen bonding within the ER $\alpha$  LBD is critical for

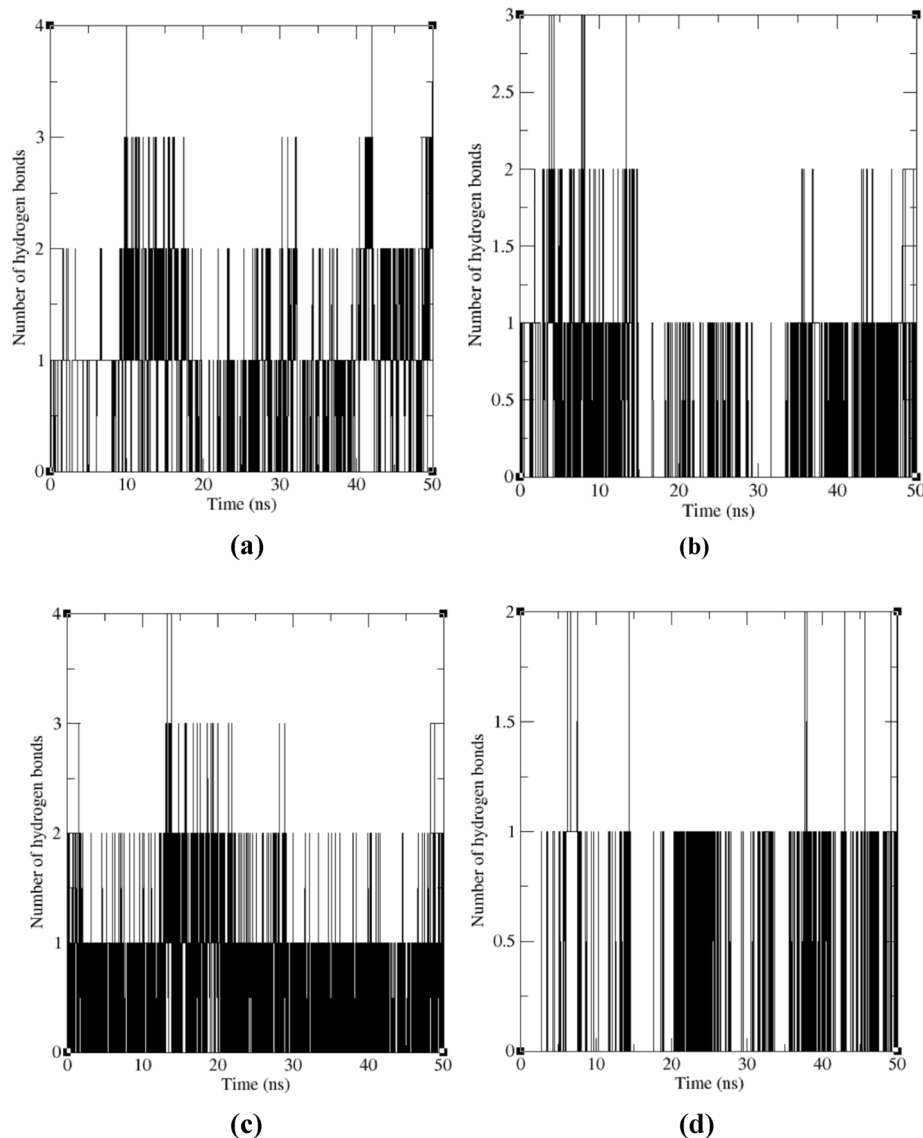


**Fig. 9** Number of hydrogen bonds formed between ER $\alpha$  and **a** Fulvestrant, **b** EED, **c** 2-Hydroxyestradiol, and **d** Ethinylestradiol during the MD simulation

antagonist activity [49], and highlight 2-Hydroxyestradiol as the analogue most capable of replicating Fulvestrant's interaction profile.

Table 5 integrates the key computational descriptors for Fulvestrant and the three selected ligands, including their docking scores, RMSD, RMSF, Rg, and hydrogen-bond interaction profiles. This consolidated presentation provides a clearer link between docking predictions, dynamic stability, and ADMET-related considerations (refer to Table 7), supporting the narrative that 2-Hydroxyestradiol maintains stability comparable to Fulvestrant, while EED and Ethinylestradiol exhibit higher flexibility and less consistent hydrogen-bonding despite their favourable docking scores.

### 3.3 Prediction of ADMET properties

A comprehensive ADMET evaluation was performed using ADMETlab 3.0 to assess both the physicochemical and pharmacokinetic properties of Fulvestrant and its

**Table 5** Comparative computational evaluation of Fulvestrant and the three top-ranked analogues, integrating docking scores, MD-derived stability metrics (RMSD, RMSF, Rg), and hydrogen-bond characteristics to guide ligand prioritization

Ligand	Docking Score (kcal/mol)	MD Stability (RMSD)	RMSF Trend	Compactness (Rg)	Hydrogen-Bond Profile
Fulvestrant	−6.49	Stable; low overall fluctuations	Moderate flexibility; low fluctuations across LBD core residues	Stable and compact	Forms 1–3 consistent H-bonds; serves as a reference stability standard
EED	−10.80	Moderate stability; larger deviations than Fulvestrant	Elevated RMSF peaks in loop regions near the binding pocket	Stable and compact	Fluctuating H-bond profile, fewer persistent H-bonds than Fulvestrant
2-Hydroxyestradiol	−10.63	Stable; very similar to Fulvestrant	RMSF pattern closely matches Fulvestrant	Stable and compact	1–2 stable H-bonds with high occupancy; comparable to Fulvestrant
Ethinylestradiol	−10.36	Moderate stability	Higher RMSF peaks across multiple regions	Stable and compact	Moderate, variably persistent H-bonds; lower dynamic stability than Fulvestrant

analogues, EED, 2-Hydroxyestradiol, and Ethinylestradiol. This analysis is important in predicting drug-likeness, metabolic behavior, systemic distribution, and toxicity liabilities, all of which are crucial in determining their suitability as therapeutic candidates [50–53]. Figure 10a–d presents radar charts of physicochemical properties for each ligand, with the orange and pink regions representing upper and lower thresholds, respectively, and the blue line denoting observed values.

Ideally, ligand properties should fall within these ranges. All four ligands demonstrated acceptable physicochemical characteristics, except for Fulvestrant, which exhibited slightly elevated logD and logP values, exceeding the recommended upper limits. In contrast, the three analogues displayed values well within the acceptable range, suggesting a more favorable physicochemical profile for drug development.

A systematic ADMET analysis was conducted to evaluate the pharmacokinetic properties, drug-likeness, and safety of Fulvestrant and its analogues, with the results summarized in Table 6 and supported by ADMETlab 3.0 predictions. In terms of absorption, all four compounds demonstrated poor predicted intestinal absorption (HIA), which is consistent with their steroidal backbone and relatively low polarity. Fulvestrant and EED showed negligible absorption probabilities ( $\leq 0.001$ ), while 2-Hydroxyestradiol (0.014) and Ethinylestradiol (0.0) displayed only marginally higher values. Distribution results showed that the steady-state volume of distribution (VDss) for all compounds was within the acceptable range (0.025–0.552 L/kg) [values not shown in Table 6], yet plasma protein binding (PPB) was uniformly high, exceeding 80% for all ligands. Fulvestrant (98.8%) and Ethinylestradiol (96.4%) exhibited the highest PPB, suggesting very low levels of free drug in circulation. Notably, Ethinylestradiol demonstrated the highest probability of blood–brain barrier (BBB) penetration at 92%, followed closely by EED and 2-Hydroxyestradiol at ~82 to 83%, whereas Fulvestrant showed relatively limited central nervous system (CNS) penetration. These findings imply that while Fulvestrant remains largely confined to systemic circulation, the analogues, particularly Ethinylestradiol, may exert effects within the CNS.

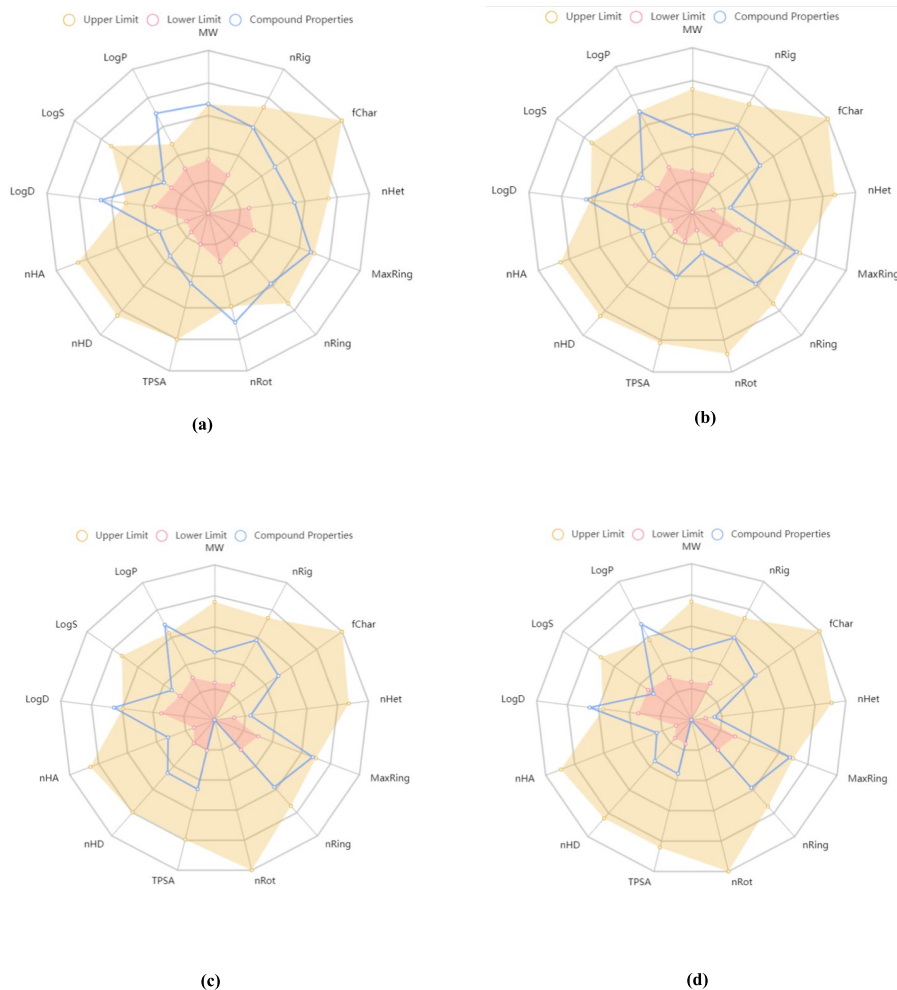


**Fig. 10** Physicochemical property radar charts for **a** Fulvestrant **b** EED **c** 2-Hydroxyestradiol, and **d** Ethinylestradiol

Toxicity predictions provided critical insights into safety of the analogues. Fulvestrant displayed the most favorable toxicity profile, with a low AMES mutagenicity probability (0.198), very low hepatotoxicity (0.105), and moderate carcinogenicity (0.652). In contrast, EED showed high AMES mutagenicity (0.596), elevated hepatotoxicity (0.669), and very high carcinogenicity (0.913), raising significant safety concerns. 2-Hydroxyestradiol exhibited moderate AMES mutagenicity (0.514), high hepatotoxicity (0.739), and high carcinogenicity (0.895), reflecting a slightly better toxicity profile compared to EED but still unfavorable relative to Fulvestrant. Ethinylestradiol displayed low mutagenicity (0.261), but very high hepatotoxicity (0.573) and carcinogenicity (0.905), which align with its well-documented tumor-promoting and hepatotoxic potential reported in the literature [54]. Although Ethinylestradiol displayed strong docking and pharmacokinetic properties, its inclusion in this study was for benchmarking purposes only. Ethinylestradiol is structurally similar to estradiol and widely used as a synthetic estrogen, making it a relevant comparator; however, its known carcinogenicity and non-genomic signaling effects preclude it from being considered as a therapeutic candidate [54].

In summary, the ADMET analysis highlights notable differences in the pharmacokinetic profiles of Fulvestrant and its analogues. Fulvestrant emerges as the safest compound, though its pharmacokinetic limitations, such as poor absorption and extremely

**Table 6** Predicted ADMET and pharmacokinetic properties of Fulvestrant and its analogues

Name of Ligand	Absorption		Distribution		Metabolism		Excretion		Toxicity	
	Intestinal Absorption		BBB	PPB	CYP		Total Clearance		AMES Mutagenicity	Hepato toxicity
	(Human)	1A2	2C19	2C9	2D6	3A4			Carcinogenicity	
[Probability of being Inhibitor (I) and Substrate (S)]										
Probability of being HIA +	Prob- ability	(%)	I	S	I	S	I	S	(ml/min/kg)	Probability of being toxic
BBB +										
Fulvestrant	0.001	0.677	98.81	0.016	0.997	0.104	0.850	0.820	0	0.150
EED	0.001	0.853	82.55	0.045	0.411	0.015	0.999	0.073	0.894	0.087
2-Hydroxyestradiol	0.014	0.950	83.15	0.044	0.929	0.001	0.987	0.153	0.803	0
Ethinylestradiol	0	0.922	96.41	0.021	1.0	1.0	1.0	0.761	0.454	0.013

Human intestinal absorption (HIA); Blood–Brain Barrier Penetration (BBB); Plasma Protein Binding (PPB)-Optimal < 90%; Cytochrome (CYP); Clearance: high (> 15 ml/min/kg); moderate (5–15 ml/min/kg); low (< 5 ml/min/kg)

high PPB, constrain its effectiveness. EED demonstrated strong docking affinity; however, it is undermined by high mutagenicity and carcinogenicity risks. 2-Hydroxyestradiol offered a more balanced profile with predictable metabolism and rapid clearance, but its high hepatotoxicity and carcinogenicity probabilities remain concerning. Ethinylestradiol stood out as pharmacokinetically attractive, given its high BBB penetration, low clearance, and relatively low mutagenicity, yet its prohibitive hepatotoxicity and carcinogenicity render it unsuitable as a therapeutic analogue. To improve clarity and facilitate direct comparison across the analogues, the key ADMET features for each compound are summarized in Table 7, highlighting their relative performance across the ADMET categories.

Although 2-Hydroxyestradiol demonstrated strong binding affinity and dynamic stability comparable to Fulvestrant, its hepatotoxicity, carcinogenicity, and rapid clearance indicate that it cannot be directly advanced as a therapeutic analogue. Instead, our findings suggest that 2-Hydroxyestradiol may serve as a lead scaffold, and future *in vitro* validation will be essential to determine whether modifications to the hydroxylated structure can retain ER $\alpha$  affinity while mitigating its reported hepatotoxicity. Furthermore, medicinal chemistry modifications (e.g., altering hydroxyl or side-chain substituents) or pro-drug/delivery strategies could enhance its pharmacokinetic profile and reduce toxicity while retaining ER $\alpha$  binding affinity. Thus, this study provides valuable computational insights into potential Fulvestrant analogues; however, the findings should be regarded as predictive rather than definitive. Future work will focus on experimental validation, beginning with *in vitro* assays such as ER $\alpha$  binding affinity measurements, cytotoxicity testing in ER+ breast cancer cell lines, and functional assays to confirm antagonistic activity. These studies, followed by *in vivo* pharmacokinetic and toxicity evaluations will be essential to establish the therapeutic relevance of the proposed analogues.

#### 4 Conclusions

In this study, an integrated *in silico* workflow comprising molecular docking, MD simulations, and ADMET prediction was employed to computationally evaluate Fulvestrant analogues for their predicted interaction with ER $\alpha$ . Among the screened compounds, EED, 2-Hydroxyestradiol, and Ethinylestradiol exhibited more favorable predicted binding affinities than Fulvestrant, with MD simulations revealing that 2-Hydroxyestradiol forms computationally stable and compact complexes comparable to Fulvestrant. ADMET analysis highlighted Fulvestrant as the safest molecule overall; however, it is computationally predicted to be limited by poor absorption and high plasma protein binding. EED demonstrated favorable docking performance but was compromised by predicted mutagenicity and carcinogenicity. In contrast, Ethinylestradiol, despite its predicted pharmacokinetic advantages, was excluded due to its known hepatotoxicity and tumor-promoting potential. Although 2-Hydroxyestradiol exhibited strong predicted binding and structural stability, its predicted hepatotoxicity, carcinogenicity, and rapid clearance suggest that it cannot be advanced directly as a therapeutic analogue. Nevertheless, its favorable computational receptor interaction profile indicates that it may serve as a lead scaffold for future optimization through structural modification or targeted delivery strategies aimed at improving its safety and pharmacokinetic characteristics.

**Table 7** Simplified ADMET profile summarizing key pharmacokinetic and toxicity characteristics of the screened ligands, indicating relative performance

Ligand	Absorption	Distribution	Metabolism	Excretion	Toxicity
Fulvestrant	Good	Poor	Moderate	Moderate	Low
EED	Good	Good	Moderate	Good	High
2-Hydroxyestradiol	Good	Good	Good	Good	High
Ethinylestradiol	Good	Poor	Poor	Moderate	High

Despite these promising computational insights, several limitations must be acknowledged. Docking scoring functions provide approximate estimates of binding affinity and may not fully capture entropic contributions or solvent effects. Similarly, the MD simulations performed here are constrained by accessible timescales and may not completely represent the long-term conformational behaviors of the ER $\alpha$ -ligand complexes. In addition, ADMET predictions are derived from statistical and machine-learning models that may not accurately reflect *in vivo* pharmacokinetic or toxicity outcomes. As all findings presented in this study are entirely *in silico*, they should be interpreted as predictive rather than confirmatory. Furthermore, docking results may be sensitive to the protonation states assigned to both ligand and receptor residues, and the 50 ns MD timescale may not fully capture slower conformational transitions of ER $\alpha$ , representing inherent limitations of the computational approach. Consequently, experimental studies are required to validate the predicted interactions and to assess the biological relevance of the identified ligands. Future work should include *in vitro* ER $\alpha$  binding assays, cytotoxicity and anti-proliferative studies in ER-positive breast cancer cell lines, and *in vivo* pharmacokinetic and toxicity evaluations to experimentally validate these computational predictions. Overall, the present study provides a strong computational framework for guiding future *in vitro* and *in vivo* investigations.

#### Acknowledgements

The authors would like to thank Indian Institute of Technology Dharwad (IIT Dharwad), India, and Visvesvaraya National Institute of Technology (VNIT) Nagpur, India for providing the infrastructural facilities to conduct the research work.

#### Author contributions

Atharva Balpande and Anushka Dashputra-Investigation, Methodology, Data Curation, Formal analysis, Validation, Writing -original draft; Nikhil Khanwani, Yashasvi Therkar and Aryan Wasewar-Investigation and Methodology; Ganesh C. Patil: Resources, Writing- review & editing; C. Ravikumar-Conceptualization, Methodology, Data Curation, Supervision, Visualization, Formal analysis, Validation, Writing -review & editing. All authors have read and agreed to the published version of the manuscript.

#### Funding

No funding was received to support this research.

#### Data availability

The corresponding author can provide data to back up the findings of this study upon reasonable request.

#### Declarations

##### Ethics approval and consent to participate

Not applicable. This study was based exclusively on computational analyses and did not involve human participants, animals, or any experimental procedures requiring ethical approval.

##### Consent for publication

Not applicable. The study does not contain any individual-level data or personally identifiable information.

##### Human or animal rights

Not applicable. No human participants were involved in this study.

##### Competing interests

The authors declare no competing interests.

Received: 7 October 2025 / Accepted: 12 January 2026

Published online: 30 January 2026

## References

1. Zhang Y, Ji Y, Liu S, Li J, Wu J, Jin Q, et al. Global burden of female breast cancer: new estimates in 2022, temporal trend and future projections up to 2050 based on the latest release from GLOBOCAN. *J Natl Cancer Cent.* 2025;5:287–96. <https://doi.org/10.1016/J.JNCC.2025.02.002>.
2. Giaquinto AN, Sung H, Newman LA, Freedman RA, Smith RA, Star J, et al. Breast cancer statistics 2024. *CA Cancer J Clin.* 2024;74(6):477–95. <https://doi.org/10.3322/CAAC.21863>.
3. Movérale-Skrtic S, Börjesson AE, Farman IH, Sjögren K, Windahl SH, Lagerquist MK, et al. The estrogen receptor antagonist ICI 182,780 can act both as an agonist and an inverse agonist when estrogen receptor α AF-2 is modified. *Proc Natl Acad Sci U S A.* 2014;111:1180–5. <https://doi.org/10.1073/PNAS.1322910111//DCSUPPLEMENTAL>.
4. Miziak P, Baran M, Blaszcak E, Przybyszewska-Podstawa A, Kalafut J, Smok-Kalwat J, et al. Estrogen receptor signaling in breast cancer. *Cancers (Basel).* 2023. <https://doi.org/10.3390/CANCERS15194689>.
5. Clusan L, Le Goff P, Flouriot G, Pakdel F. A closer look at estrogen receptor mutations in breast cancer and their implications for estrogen and antiestrogen responses. *Int J Mol Sci.* 2021;22:1–16. <https://doi.org/10.3390/IJMS22020756>.
6. Porras L, Ismail H, Mader S. Positive regulation of estrogen receptor alpha in breast tumorigenesis. *Cells.* 2021. <https://doi.org/10.3390/CELLS10112966>.
7. Strillacci A, Sansone P, Rajasekhar VK, Turkekul M, Boyko V, Meng F, et al. ERα-LBD, an isoform of estrogen receptor alpha, promotes breast cancer proliferation and endocrine resistance. *NPJ Breast Cancer.* 2022;2022 81:8:1–16. <https://doi.org/10.1038/s41523-022-00470-6>.
8. Johnston SJ, Cheung K-L. Endocrine therapy for breast cancer: a model of hormonal manipulation. *Oncol Ther.* 2018. <https://doi.org/10.1007/S40487-018-0062-X>.
9. McKeage K, Curran MP, Plosker GL. Fulvestrant: a review of its use in hormone receptor-positive metastatic breast cancer in postmenopausal women with disease progression following antiestrogen therapy. *Drugs.* 2004;64:633–48. <https://doi.org/10.2165/00003495-200464060-00009>.
10. Li J, Wang Z, Shao Z. Fulvestrant in the treatment of hormone receptor-positive/human epidermal growth factor receptor 2-negative advanced breast cancer: a review. *Cancer Med.* 2019;8:1943. <https://doi.org/10.1002/CAM4.2095>.
11. Schmid MRN. A review of fulvestrant in breast cancer. *Oncol Ther.* 2017. <https://doi.org/10.1007/s40487-017-0046-2>.
12. Rocca A, Maltoni R, Bravaccini S, Donati C, Andreis D. Clinical utility of fulvestrant in the treatment of breast cancer: a report on the emerging clinical evidence. *Cancer Manag Res.* 2018;10:3083. <https://doi.org/10.2147/CMAR.S137772>.
13. Carlson RW. The history and mechanism of action of fulvestrant. *Clin Breast Cancer.* 2005;6(Suppl 1):S5. <https://doi.org/10.3816/CBC.2005.S.008>.
14. Hernando C, Ortega-Morillo B, Tapia M, Moragón S, Martínez MT, Eroles P, et al. Oral selective estrogen receptor degraders (SERDs) as a novel breast cancer therapy: present and future from a clinical perspective. *Int J Mol Sci.* 2021. <https://doi.org/10.3390/IJMS22157812>.
15. Pancholi S, Simigdala N, Ribas R, Schuster E, Ferreira Leal M, Nikitorowicz-Buniak J, et al. Elacestrant demonstrates strong anti-estrogenic activity in PDX models of estrogen-receptor positive endocrine-resistant and fulvestrant-resistant breast cancer. *NPJ Breast Cancer.* 2022. <https://doi.org/10.1038/s41523-022-00483-1>.
16. Mottamal M, Kang B, Peng X, Wang G. From pure antagonists to pure degraders of the estrogen receptor: evolving strategies for the same target. *ACS Omega.* 2021;6:9334. <https://doi.org/10.1021/ACOSOMEA.OC06362>.
17. Vallet A, Diennet M, Thiombane K, Vivet A, Weber S, El Ezzy M, et al. OR11-02 structural determinants of pure antiestrogenic activity. *J Endocr Soc.* 2023. <https://doi.org/10.1210/JENDSO/BVAD114.1735>.
18. Stivala LA, Savio M, Carafoli F, Perucca P, Bianchi L, Maga G, et al. Specific structural determinants are responsible for the antioxidant activity and the cell cycle effects of resveratrol. *J Biol Chem.* 2001;276:22586–94. <https://doi.org/10.1074/JBC.M101846200>.
19. Hulme EC, Trevethick MA. Ligand binding assays at equilibrium: validation and interpretation. *Br J Pharmacol.* 2010;161:1219. <https://doi.org/10.1111/J.1476-5381.2009.00604.X>.
20. Hong H, Brannah WS, Ng HW, Moland CL, Dial SL, Fang H, et al. Human sex hormone-binding globulin binding affinities of 125 structurally diverse chemicals and comparison with their binding to androgen receptor, estrogen receptor, and α-fetoprotein. *Toxicol Sci.* 2015;143:333–48. <https://doi.org/10.1093/TOXSCI/KFU231>.
21. Yao J, Tao Y, Hu Z, Li J, Xue Z, Zhang Y, et al. Optimization of small molecule degraders and antagonists for targeting estrogen receptor based on breast cancer: current status and future. *Front Pharmacol.* 2023;14:1225951. <https://doi.org/10.3389/FPHAR.2023.1225951>.
22. Kurtanović N, Tomašević N, Matić S, Proia E, Sabatino M, Antonini L, et al. Human estrogen receptor alpha antagonists, part 3: 3-D pharmacophore and 3-D QSAR guided brefeldin A hit-to-lead optimization toward new breast cancer suppressants. *Molecules.* 2022;27:2823. <https://doi.org/10.3390/MOLECULES27092823/S1>.
23. Rodríguez-Macías J, Saurith-Coronell O, Vargas-Echeverría C, Delgado DL, Márquez-Brazón EA, De Aguas RG, et al. Multitarget design of steroidal inhibitors against hormone-dependent breast cancer: an integrated *in silico* approach. *Int J Mol Sci.* 2025;26:7477. <https://doi.org/10.3390/IJMS26157477/S1>.
24. Shagupta I, Ahmad S, Mathew S, Rahman S. Recent progress in selective estrogen receptor downregulators (SERDs) for the treatment of breast cancer. *RSC Med Chem.* 2020;11:438. <https://doi.org/10.1039/C9MD00570>.
25. Pandiyan S, Wang L. A comparative study of Bazedoxifene, Exemestane, Fulvestrant, Raloxifene, Tryprostatin A, and Vorinostat compounds as potential inhibitors against breast cancer through molecular docking, and molecular dynamics simulation. *Chin J Anal Chem.* 2023;51:100315. <https://doi.org/10.1016/J.CJAC.2023.100315>.
26. Guo S, Zhang C, Bratton M, Mottamal M, Liu J, Ma P, et al. ZB716, a steroidal selective estrogen receptor degrader (SERD), is orally efficacious in blocking tumor growth in mouse xenograft models. *Oncotarget.* 2018;9:6924–37. <https://doi.org/10.18633/ONCOTARGET.24023>.
27. Wishart DS, Feunang YD, Guo AC, Lo EJ, Marcu A, Grant JR, et al. DrugBank 5.0: a major update to the DrugBank database for 2018. *Nucleic Acids Res.* 2018;46:D1074–82. <https://doi.org/10.1093/NAR/GKX1037>.
28. Dashputra A, Therkar Y, Balpande A, Khanwani N, Wasewar A, Patil GC, et al. Evaluation of tamoxifen analogues as potential estrogen receptor alpha inhibitors for breast cancer treatment: a computational approach. *J Mol Liq.* 2024;414:126209. <https://doi.org/10.1016/J.MOLLIQ.2024.126209>.
29. Bennett CH. Efficient estimation of free energy differences from Monte Carlo data. *J Comput Phys.* 1976;22:245–68. [https://doi.org/10.1016/0021-9991\(76\)90078-4](https://doi.org/10.1016/0021-9991(76)90078-4).

30. Meng X-Y, Zhang H-X, Mezei M, Cui M. Molecular docking: a powerful approach for structure-based drug discovery. *Curr Comput Aided Drug Des.* 2012;7:146–57. <https://doi.org/10.2174/157340911795677602>.
31. Taghizadeh MS, Niazi A, Moghadam A, Afsharifar A. Experimental, molecular docking and molecular dynamic studies of natural products targeting overexpressed receptors in breast cancer. *PLoS ONE.* 2022;17:e0267961. <https://doi.org/10.1371/JOURNAL.PONE.0267961>.
32. Agu PC, Afiukwa CA, Orji OU, Ezeh EM, Ofoke IH, Ogbu CO, et al. Molecular docking as a tool for the discovery of molecular targets of nutraceuticals in diseases management. *Sci Rep.* 2023;2023(1):1–18. <https://doi.org/10.1038/s41598-023-4016-0-2>.
33. O'Boyle NM, Banck M, James CA, Morley C, Vandermeersch T, Hutchison GR. Open Babel: an open chemical toolbox. *J Cheminform.* 2011. <https://doi.org/10.1186/1758-2946-3-33>.
34. BIOVIA, Dassault Systèmes, BIOVIA Discovery Studio, 2020, San Diego: Dassault Systèmes 2020., 2020.
35. Sinyani A, Idowu K, Shunmugam L, Kumalo HM, Khan R. A molecular dynamics perspective into estrogen receptor inhibition by selective flavonoids as alternative therapeutic options. *J Biomol Struct Dyn.* 2023;41:4093–105. <https://doi.org/10.1080/07391102.2022.2062786>.
36. Abraham M, Alekseenko A, Bergh C, Blau C, Briand E, Doijade M, Fleischmann S, Gapsys V, Garg G, Gorelov S, Gouaillardet G, Gray A, Irrgang ME, Jalalypour F, Jordan J, Junghans C, Kanduri P, Keller S, Kutzner C, Lemkul JA, Lundborg M, Merz P, Miletic V, Morozov D, Päll S, Schulz R, Shirts M, Shvetsov A, Soproni B, van der Spoel D, Turner P, Uphoff C, Villa A, Wingbermühle S, Zhmurov A, Bauer P, Hess B, Lindahl E, GROMACS 2023 Manual, (n.d.). <https://doi.org/10.5281/ZENODO.7588711>.
37. Chen D, Oezguen N, Urvil P, Ferguson C, Dann SM, Savidge TC. Regulation of protein-ligand binding affinity by hydrogen bond pairing. *Sci Adv.* 2016. [https://doi.org/10.1126/SCIADV.1501240/SUPPL\\_FILE/1501240\\_SM.PDF](https://doi.org/10.1126/SCIADV.1501240/SUPPL_FILE/1501240_SM.PDF).
38. Mohamed NM, Ali EMH, Aboulmagd AM. Ligand-based design, molecular dynamics and ADMET studies of suggested SARS-CoV-2 Mpro inhibitors. *RSC Adv.* 2021;11:4523–38. <https://doi.org/10.1039/DORA10141A>.
39. Jiang D, Lei T, Wang Z, Shen C, Cao D, Hou T. ADMET evaluation in drug discovery. 20. Prediction of breast cancer resistance protein inhibition through machine learning. *J Cheminformatics.* 2020;2020(1):1–26. <https://doi.org/10.1186/S1332-1-020-00421-Y>.
40. Flores-Holguín N, Frau J, Glossman-Mitnik D. Computational pharmacokinetics report, ADMET study and conceptual DFT-based estimation of the chemical reactivity properties of marine cyclopeptides. *ChemistryOpen.* 2021;10:1142. <https://doi.org/10.1002/OPEN.202100178>.
41. Xiong G, Wu Z, Yi J, Fu L, Yang Z, Hsieh C, et al. ADMETlab 2.0: an integrated online platform for accurate and comprehensive predictions of ADMET properties. *Nucleic Acids Res.* 2021;49:W5. <https://doi.org/10.1093/NAR/GKAB255>.
42. Fluoroestradiol F-18 | C18H23FO2 | CID 10869981 - PubChem, (n.d.). <https://pubchem.ncbi.nlm.nih.gov/compound/Fluoroestradiol-F-18> Accessed 13 Nov 2025.
43. Sreekumar S, Kuthe AM, Tripathi SC, Patil GC, Ravikumar C. Integrated computational approach towards identification of HSPG and ACE2 mimicking moieties for SARS-CoV-2 inhibition. *J Mol Liq.* 2022;367:120566. <https://doi.org/10.1016/j.molliq.2022.120566>.
44. Muhseen ZT, Hameed AR, Al-Hasani HMH, ul Qamar MT, Li G. Promising terpenes as SARS-CoV-2 spike receptor-binding domain (RBD) attachment inhibitors to the human ACE2 receptor: integrated computational approach. *J Mol Liq.* 2020. <https://doi.org/10.1016/J.MOLLIQ.2020.114493>.
45. Pinzone JJ, Stevenson H, Strobl JS, Berg PE. Molecular and cellular determinants of estrogen receptor α expression. *Mol Cell Biol.* 2004;24:4605–12. [https://doi.org/10.1128/MCB.24.11.4605-4612.2004.FPPNG](https://doi.org/10.1128/MCB.24.11.4605-4612.2004/ASSET//CMS/ASSET/9CE95F36-C95E-4B1F-BCEB-9E76310D9A1D/MCB.24.11.4605-4612.2004.FPPNG).
46. Rane JS, Pandey P, Chatterjee A, Khan R, Kumar A, Prakash A, et al. Targeting virus–host interaction by novel pyrimidine derivative: an in silico approach towards discovery of potential drug against COVID-19. *J Biomol Struct Dyn.* 2020;39:1–11. <https://doi.org/10.1080/07391102.2020.1794969>.
47. Bitencourt-Ferreira G, Veit-Acosta M, de Azevedo WF. Hydrogen bonds in protein-ligand complexes. *Methods Mol Biol.* 2019;2053:93–107. [https://doi.org/10.1007/978-1-4939-9752-7\\_7](https://doi.org/10.1007/978-1-4939-9752-7_7).
48. Karthick V, Nagasundaram N, Doss CGP, Chakraborty C, Siva R, Lu A, et al. Virtual screening of the inhibitors targeting at the viral protein 40 of Ebola virus. *Infect Dis Poverty.* 2016;5:1–10. <https://doi.org/10.1186/S40249-016-0105-1/FIGURES/10>.
49. Gangloff M, Ruff M, Eiler S, Duclaud S, Wurtz JM, Moras D. Crystal structure of a mutant hERα ligand-binding domain reveals key structural features for the mechanism of partial agonism. *J Biol Chem.* 2001;276:15059–65. <https://doi.org/10.1074/jbc.M009870200>.
50. Dulsat J, López-Nieto B, Estrada-Tejedor R, Borrell JI. Evaluation of free online ADMET tools for academic or small biotech environments. *Molecules.* 2023. <https://doi.org/10.3390/MOLECULES28020776/S1>.
51. Ahmad I, Kuznetsov AE, Pirzada AS, Alsharif KF, Daglia M, Khan H. Computational pharmacology and computational chemistry of 4-hydroxyisoleucine: physicochemical, pharmacokinetic, and DFT-based approaches. *Front Chem.* 2023. <https://doi.org/10.3389/FCHEM.2023.1145974>.
52. Ahmad I, Khan H, Serdaroglu G. Physicochemical properties, drug likeness, ADMET, DFT studies, and in vitro antioxidant activity of oxindole derivatives. *Comput Biol Chem.* 2023;104:107861. <https://doi.org/10.1016/J.COMPBIOLCHEM.2023.107861>.
53. El Fadili M, Er-Rajy M, Kara M, Assouguem A, Belhassan A, Alotaibi A, et al. QSAR, ADMET in silico pharmacokinetics, molecular docking and molecular dynamics studies of novel bicyclo (aryl methyl) benzamides as potent GlyT1 inhibitors for the treatment of schizophrenia. *Pharmaceutics (Basel).* 2022. <https://doi.org/10.3390/PH15060670>.
54. Beaver EF, Malone KE, Tang MTC, Barlow WE, Porter PL, Daling JR, et al. Oral contraceptives and breast cancer risk overall and by molecular subtype among young women. *Cancer Epidemiol Biomarkers Prev.* 2014;23:755–64. <https://doi.org/10.1158/1055-9965.EPI-13-0944/67631/AM/ORAL-CONTRACEPTIVES-AND-BREAST-CANCER-RISK-OVERALL>.

## Publisher's Note

Springer Nature remains neutral with regard to jurisdictional claims in published maps and institutional affiliations.